The 9th European Congress on Computational Methods in Applied Sciences and Engineering
ECCOMAS Congress 2024
3–7 June 2024, Lisboa, Portugal

WOOD CONSTITUTIVE LAW IMPLEMENTATION IN FINITE ELEMENT SOFTWARE ZSOIL TO MODEL DOWEL EMBEDMENT TESTS ON GLULAM

MARGAUX DELAGE[1,2], GIL JACOT-DESCOMBES[1], DAMIEN SCANTAMBURLO[2] AND STEPHANE COMMEND[1,3]

[1] GeoMod ingénieurs conseils SA
Epinettes 32, 1007 Lausanne, Switzerland
e-mail: {mdelage,gjdescombes,scommend}@geomod.ch, www.geomod.ch

[2] MONOD – PIGUET + ASSOCIES Ingénieurs Conseils SA
Avenue de Cour 32, 1007 Lausanne, Switzerland
e-mail: damien.scantamburlo@mpaic.com, www.mpaic.com

[3] School of Engineering and Architecture, HES-SO
Boulevard de Pérolles 80, 1700 Fribourg, Switzerland
www.hes-so.ch

Key words: Wood, Continuum damage mechanics, Orthotropy, Numerical finite element simulation, Bayesian inversion

Summary. This paper presents three-dimensional finite element simulations of wood specimens and dowel embedment tests using an elastic-plastic and damage model in order to simulate the nonlinear behaviour of wood interacting with a metal connection. The wood constitutive law relies upon orthotropic material parameters, associated plasticity and continuum damage mechanics (CDM) to take into account the following properties of wood : anisotropy, brittle failure in tension, plasticity and ductile failure in compression. The model used in this paper is implemented as a user subroutine of the finite element software ZSoil. The material parameters of the model are determined through a Bayesian inversion analysis based on experimental and numerical data from uniaxial compression tests on glulam samples. The constitutive model with the calibrated material parameters are used to numerically simulate dowel embedment experimental tests on glulam. The results demonstrate the model's capability to reasonably approximate embedment tests and the nonlinear behaviour of wood, opening up interesting prospects for engineers to better understand and optimize structures.

1 INTRODUCTION

Wood is a material increasingly used in the construction field for its interesting mechanical properties and environmental benefits. Most wooden structures use a variety of joining methods, from contact joints (dowel) to friction techniques (threaded rods). Modelling these structures remains challenging due to the non-linear and anisotropic behaviour of wood coupled with the complex phenomenon of wood-steel interaction, which leads to applying high security factors when designing structures. Simulating the complex mechanical properties of wood is then key to

predict the behaviour of wooden structures. Do to its fibrous structure, wood is an anisotropic material that can develop, depending on the load direction, plasticity or failure.

Finite element method provides interesting tools to model nonlinear material. Through the implementation of plastic theory or Continuum Damage Mechanics (CDM) in FE-models, several constitutive laws have been developed specifically for wood. To trigger nonlinear behaviour, various criteria have been employed including Hill criterion [1] which does not take into account the asymmetry between tension and compression. This can be solved by using other criteria such as Hoffman [2] or Tsai-Wu [3]. Besides the aforementioned polynomial criteria, another approach is to use several failure criteria to detect different failure modes. Sandhaas et al. [4] proposed an orthotropic model using four damage modes and a damage variable to imitate plasticity. Other models [5, 6, 7] introduced plasticity algorithm in addition to continuum damage mechanics to perform cyclic loading of the material.

In this paper, a constitutive 3D model for wood is developed taken into account a plastic behaviour in compression initiatied by the Hoffman criterion. Four damage variables are also incorporated to captures different failure modes. The constitutive model was implemented as a user-subroutine in the finite-element software ZSoil [8]. This constitutive law involves a lot of material parameters to calibrate the non-linear behaviour. These parameters are usually not provided by standard wood characterization, that is why this article proposes a method using metamodels and Bayesian inversion to calibrate the material parameters on basic tests. This analysis is performed using the uncertainty quantification software UQLab [9]. The constitutive law and its calibrated parameters are then employed in dowel-embedment tests to reproduce experimental results.

2 THE CONSTITUTIVE MODEL FOR WOOD

2.1 Stress-strain relationship

Wood is assumed to be an orthotropic material with three principal directions defined with respect to grain direction and growth rings. Fig. 1 shows these three directions: longitudinal (L), radial (R) and tangential (T). Considering wood has quite similar mechanical behaviour along the radial and tangential directions by comparison to the longitudinal direction, same material properties are set for directions R and T in this paper even if the implemented law is orthotropic.

Continuum damage mechanics (CDM) has been used to model cracks in material matrix and thus, nonlinear brittle failure. Some models for wood have been developed using this theory [4, 6]. CDM introduces an effective stress tensor to quantify undamaged material matrix stress state while the Cauchy tensor quantifies the stress state of the damaged material. Then, according to the concept of strain equivalence [10, 11], the effective stress tensor $\bar{\boldsymbol{\sigma}}$ can be related to the strain tensor using the fundamental Hooke equation:

$$\bar{\boldsymbol{\sigma}} = \mathbf{D_0} : \boldsymbol{\varepsilon}^e \tag{1}$$

With $\mathbf{D_0}$ being the stiffness tensor for the undamaged wood. The Cauchy stress tensor $\boldsymbol{\sigma}$ is related to the effective stress tensor by means of a damage tensor $\mathbf{M}(d)$ which depends on the damage state d. Consequently, the Cauchy stress tensor can be related to the strain tensor by

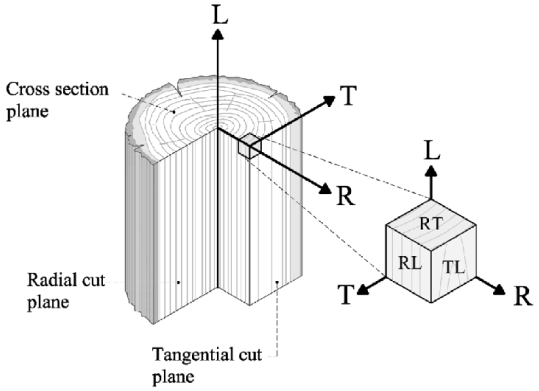

Figure 1: Definition of material directions in wood matrix

use of a tensor noted $\mathbf{D_{dam}}$ using equations (2):

$$\boldsymbol{\sigma} = \mathbf{M}(d) : \bar{\boldsymbol{\sigma}} \quad ; \quad \boldsymbol{\sigma} = \mathbf{D_{dam}} : \varepsilon^e \tag{2}$$

Since wood is considered an orthotropic material in this paper, the stiffness tensor in Voigt's notation is expressed as :

$$\mathbf{D_0} = \begin{bmatrix} \frac{E_L(1-\nu_{RT}\nu_{TR})}{\Delta} & \frac{E_L(\nu_{RL}+\nu_{TL}\nu_{RT})}{\Delta} & \frac{E_L(\nu_{TL}+\nu_{RL}\nu_{TR})}{\Delta} & 0 & 0 & 0 \\ \frac{E_R(\nu_{LR}+\nu_{TR}\nu_{LT})}{\Delta} & \frac{E_R(1-\nu_{LT}\nu_{TL})}{\Delta} & \frac{E_R(\nu_{TR}+\nu_{LR}\nu_{TL})}{\Delta} & 0 & 0 & 0 \\ \frac{E_T(\nu_{LT}+\nu_{RT}\nu_{LR})}{\Delta} & \frac{E_T(\nu_{RT}+\nu_{LT}\nu_{RL})}{\Delta} & \frac{E_T(1-\nu_{LR}\nu_{RL})}{\Delta} & 0 & 0 & 0 \\ 0 & 0 & 0 & G_{RT} & 0 & 0 \\ 0 & 0 & 0 & 0 & G_{TL} & 0 \\ 0 & 0 & 0 & 0 & 0 & G_{LR} \end{bmatrix} \tag{3}$$

$$\Delta = 1 - \nu_{LR}\nu_{RL} - \nu_{RT}\nu_{TR} - \nu_{LT}\nu_{TL} - 2\nu_{RL}\nu_{TR}\nu_{LT}$$

2.2 Effective stress tensor decomposition

Given the plasticity occurs in wood only by compression of the fibres, it is chosen to separate the compressive ($\bar{\boldsymbol{\sigma}}^-$) and the tensile ($\bar{\boldsymbol{\sigma}}^+$) components of the effective stress using Eq. (4) [6] to evaluate plasticity evolution on the compressive part only.

$$\bar{\boldsymbol{\sigma}}^+ = \sum_{i=1}^{3} \langle \bar{\sigma}_i \rangle \mathbf{p}_i \otimes \mathbf{p}_i \quad ; \quad \bar{\boldsymbol{\sigma}}^- = \bar{\boldsymbol{\sigma}} - \bar{\boldsymbol{\sigma}}^+ \tag{4}$$

Where $\mathbf{p}_i$ and $\langle \bar{\sigma}_i \rangle$ are the eigenvectors and eigenvalues respectively.

2.3 Plasticity algorithm

The plastic evolution is applied to the effective space and, as said in previous section, to the compressive effective stress tensor $\bar{\boldsymbol{\sigma}}^-$ only. The plastic model here is taken from Sirumbal-Zapata's work [6]. The plasticity is triggered by Hoffman yield criterion [2] applied on the compressive effective stress:

$$f_p = \frac{1}{2}\bar{\boldsymbol{\sigma}}^{-\intercal}\boldsymbol{P}\bar{\boldsymbol{\sigma}}^- + \bar{\boldsymbol{\sigma}}^{-\intercal}\boldsymbol{q}(k) - \bar{\sigma}_y^2(k) \geq 0 \tag{5}$$

with :

$$\mathbf{P} = \begin{pmatrix} \chi_1 & -\chi_4 & -\chi_5 & 0 & 0 & 0 \\ -\chi_4 & \chi_2 & -\chi_6 & 0 & 0 & 0 \\ -\chi_5 & -\chi_6 & \chi_3 & 0 & 0 & 0 \\ 0 & 0 & 0 & \chi_7 & 0 & 0 \\ 0 & 0 & 0 & 0 & \chi_8 & 0 \\ 0 & 0 & 0 & 0 & 0 & \chi_9 \end{pmatrix} \quad ; \quad \mathbf{q}(k) = \bar{\sigma}_y(k) \begin{pmatrix} \chi_{10} \\ \chi_{11} \\ \chi_{12} \\ 0 \\ 0 \\ 0 \end{pmatrix} \tag{6}$$

and the following coefficients:

$$\begin{cases} \chi_1 = \frac{2}{f_L^+ f_L^-} & \chi_2 = \frac{2}{f_R^+ f_R^-} & \chi_3 = \frac{2}{f_T^+ f_T^-} \\ \chi_4 = -\frac{1}{2}\left(\chi_1 + \chi_2 - \chi_3\right) & \chi_5 = -\frac{1}{2}\left(\chi_1 - \chi_2 + \chi_3\right) & \chi_6 = -\frac{1}{2}\left(-\chi_1 + \chi_2 + \chi_3\right) \\ \chi_7 = \frac{2}{f_{LR}^2} & \chi_8 = \frac{2}{f_{RT}^2} & \chi_9 = \frac{2}{f_{TL}^2} \\ \chi_{10} = \frac{f_L^- - f_L^+}{f_L^+ f_L^-} & \chi_{LL} = \frac{f_R^- - f_R^+}{f_R^+ f_R^-} & \chi_{LR} = \frac{f_T^- - f_T^+}{f_T^+ f_T^-} \end{cases} \tag{7}$$

The reference yield stress is defined as: $\bar{\sigma}_y(k) = \bar{\sigma}_{y,0}(k) + hk$ where h is the hardening moduli of the material and k is the isotropic hardening variable. The initial value of the reference yield stress is $\bar{\sigma}_{y,0}(k) = 1$.

The associated plastic flow rule is given as:

$$\dot{\boldsymbol{\varepsilon}}^p = \dot{\lambda}\boldsymbol{n}(\bar{\boldsymbol{\sigma}}^-, k) \quad ; \quad \boldsymbol{n} = \left(\frac{\partial f_p(\bar{\boldsymbol{\sigma}}^-, k)}{\partial \bar{\boldsymbol{\sigma}}^-}\right)^{\intercal} = \boldsymbol{P}\bar{\boldsymbol{\sigma}}^- + \boldsymbol{q}(k) \tag{8}$$

and the isotropic hardening variable k is obtained with:

$$\dot{k} = \dot{\lambda}\sqrt{\boldsymbol{n}^{\intercal}\boldsymbol{T}\boldsymbol{n}} \quad ; \quad \boldsymbol{T} = \mathrm{diag}[1, 1, 1, 1/2, 1/2, 1/2] \tag{9}$$

2.4 Damage model

The failure of wood creates cracks and voids in the material matrix, leading to a degradation of the material properties. Continuum Damage Mechanics proposes to degrade the material through decrease of the parameters of the stiffness tensor. In order to take into account four different failure modes, four damage function $d_{i,c/t}$ and damage criterion $F_{i,c/t}$ are introduced [4, 5]:

$$\begin{aligned} &\bar{\sigma}_{LL} \leq 0, \quad F_{L,c} = -\frac{\bar{\sigma}_{LL}}{f_L^t} - 1 \geq 0 \\ &\bar{\sigma}_{LL} \geq 0, \quad F_{L,t} = \frac{\bar{\sigma}_{LL}}{f_L^t} - 1 \geq 0 \\ &\bar{\sigma}_{RR} \geq 0, \quad F_{R,t} = \left(\frac{\bar{\sigma}_{RR}}{f_R^t}\right)^2 + \left(\frac{\bar{\sigma}_{LT}}{f_{LR}^s}\right)^2 + \left(\frac{\bar{\sigma}_{RT}}{f_{RT}^s}\right)^2 - 1 \geq 0 \\ &\bar{\sigma}_{TT} \geq 0, \quad F_{T,t} = \left(\frac{\bar{\sigma}_{TT}}{f_T^t}\right)^2 + \left(\frac{\bar{\sigma}_{LT}}{f_{LT}^s}\right)^2 + \left(\frac{\bar{\sigma}_{RT}}{f_{RT}^s}\right)^2 - 1 \geq 0 \end{aligned} \tag{10}$$

When the damage criteria are met, damage functions are updated to weaken the wood. Damage functions $d_{i,c/t}$ take values between 0 and 1, 0 being the undamaged state and 1 the

fully damaged state. The material is supposed to be undamaged at initial step : $d^0_{i,c/t} = 0$. The three damage functions for tensile failure follow an exponential degradation model and are then defined for each new time step $n+1$ as follows :

$$\begin{aligned} d_{i,t} &= 1 - \frac{1}{F_{i,t}} \exp\left((1 - F_{i,t}) \frac{L_c f_i^{t\,2}}{E_i G_{f,i}} \right) \quad \text{with } i = L, R, T \\ d_{i,t}^{n+1} &= max(d_{i,t}, d_{i,t}^n) \end{aligned} \tag{11}$$

where the crack band method [12] is introduced to reduce mesh-dependency issues by using the characterist length of the element L_c which is defined as the cubic root of the element's volume: $L_c = \sqrt[3]{V_e}$. The discretized equation of damage is taking the maximum value at each step to enforce the irreversibility of damage in the material matrix.

The compressive damage function is expressed as follows:

$$\begin{aligned} d_{Lc} &= 1 - \frac{1}{F_{L,c}}(1 - A) - A \exp\left(B(1 - F_{L,c})\right) \\ d_{L,c}^{n+1} &= max(d_{L,c}, d_{L,c}^n) \end{aligned} \tag{12}$$

where parameters A and B are calibrated thanks to material tests.

The damage tensor $\mathbf{M}(d)$ is then expressed as follows [13] and induces a degradation of the stiffness tensor $\mathbf{D_0}$ into $\mathbf{D_{dam}}$ according to Eq. (2).

$$\begin{aligned} \mathbf{M(d)} = \text{diag}([\,&(1 - d_L),\, (1 - d_R),\, (1 - d_T), \\ &\sqrt{(1 - d_R)(1 - d_T)},\, \sqrt{(1 - d_L)(1 - d_T)},\, \sqrt{(1 - d_L)(1 - d_R)}\,]) \end{aligned} \tag{13}$$

2.5 Viscous regularization

The constitutive law can encounter convergence issues because of the introduction of damage variables. To improve the convergence of the algorithm, a viscous regularization is applied to the damage variables, following the technique proposed by Duvaut and Lions [14] and discretized:

$$\dot{d}^v = \frac{1}{\eta}(d - d^v) \quad ; \quad d^v_{n+1} = \frac{\eta}{\eta + \Delta t} d^v_n + \frac{\Delta t}{\eta + \Delta t} d_{n+1} \tag{14}$$

3 NUMERICAL IMPLEMENTATION

The subroutine is implemented on the finite element software ZSoil [8] through the user development module which allows the user to implement new constitutive laws. The algorithm is taking an increment of strain as input along with the values of the previous step. Fig. 2 shows the flow diagram of the material subroutine.

The algorithm first calculates a trial effective stress by Hooke's law (Eq. (1)) using the previous effective stress tensor and the increment of strain. Then, this trial effective stress tensor is decomposed to extract the compressive part (Eq. (4)) which will be used to evaluate the value of the yield function (Eq. (5)). If the yield function signals plasticity, a Newton-Raphson algorithm is run to determine the compressive effective stress tensor and the plastic

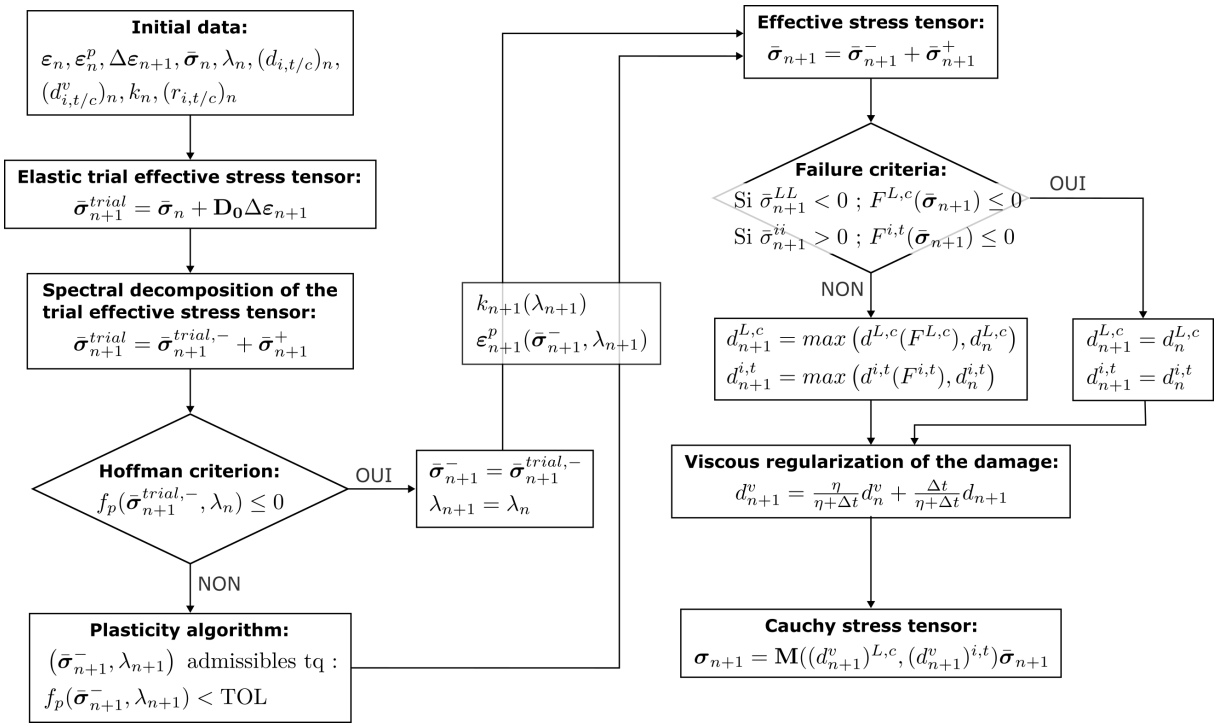

Figure 2: Flowchart of the material subroutine

strain increment. Otherwise, the trial effective stress tensor is considered the effective stress tensor.

The effective stress tensor is then used to calculate the Cauchy stress tensor (Eq. (2)). In order to build the damage tensor $\mathbf{M}(d)$, the algorithm checks the four failure criterion (Eq. (10)) and calculate the corresponding damage variables if necessary (Eq. (11) and Eq. (12)). The damage variables are slightly modified thanks to viscous regularization (Eq. (14)) to improve numerical convergence. The damage tensor is then calculated (Eq. (13)) and is used to find the Cauchy stress tensor.

The subroutine keeps in memory the following material parameters for next step : the effective stress tensor $\bar{\boldsymbol{\sigma}}_{n+1}$, the Cauchy stress tensor $\boldsymbol{\sigma}_{n+1}$, the total plastic strain $\boldsymbol{\varepsilon}^p_{n+1}$, the damage variables $d_{i,n+1}$,the viscous damage variables $d^v_{i,n+1}$, the plastic multiplier λ_{n+1}, the isotropic hardening variable k_{n+1}.

4 EXPERIMENTAL VALIDATION

In this section, the implemented constitutive law is evaluated on experimental tests from Karagiannis et al. [15]. First, thanks to the material characterization tests (see Fig. 3), the material parameters of wood are calibrated with help of a Bayesian analysis. Then, the output parameters from the calibration are injected in the finite element models of Fig. 5 to try to reproduce the experimental results.

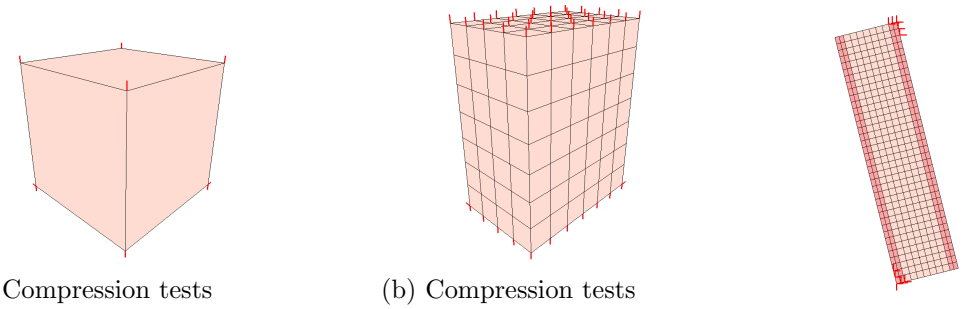

(a) Compression tests parallel to the grain

(b) Compression tests perpendicular to the grain

(c) Shear test

Figure 3: Finite-element wood samples loaded in compression in three different directions

4.1 Parameter calibration

The material characterization tests are performed using ZSoil finite element models simulating three types of loading to test the material in three directions (Fig. 3): parallel to the grain (Fig. 3a), perpendicular to the grain (Fig. 3b) and with a 14° angle with respect to the grain direction (Fig. 3c). To calibrate the material parameters for each of the three characterization tests, a Bayesian inversion is performed using as observation data 4 points of the experimental stress-strain curves. To reduce the computational costs, a PCE approximating the ZSoil model response is created and then used in the Bayesian inversion process. As shown in Fig.4, the calibrated material parameters match the stress-strain curve for each of the chosen observation point.

The resulting material parameters from the Bayesian calibration are listed below in Table. 1.

Table 1: Calibrated material parameters' value

Young's moduli [MPa]	$E_L = 2022.8$	$E_R = 165.4$	$E_T = 165.4$
Shear moduli [MPa]	$G_{LR} = 167.8$	$G_{RT} = 58.3$	$G_{TL} = 167.8$
Poisson's ratio	$\nu_{LR} = 0.31$	$\nu_{RT} = 0.42$	$\nu_{TL} = 0.06$
Tensile strength [MPa]	$f_L^+ = 21.93$	$f_R^+ = 0.79$	$f_T^+ = 0.79$
Compressive strength [MPa]	$f_L^- = 38.88$	$f_R^- = 1.78$	$f_T^- = 1.78$
Shear strength [MPa]	$f_{LR} = 6.05$	$f_{RT} = 0.46$	$f_{TL} = 6.05$
Fracture energy density [N/mm]	$G_{f,L} = 68.6$	$G_{f,R} = 7.5$	$G_{f,T} = 7.5$
Hardening modulus		$h = 1.8$	
Softening parameter A		$A = 0.58$	
Softening parameter B		$B = 0.86$	

4.2 Results on dowel-embedment tests

The material's constitutive law and the calibrated parameters summarized in Table. 1 are used as inputs for dowel-embedment tests experimentally performed by Karagiannis [15] with the same spruce glulam as the characterization tests on Fig. 3.

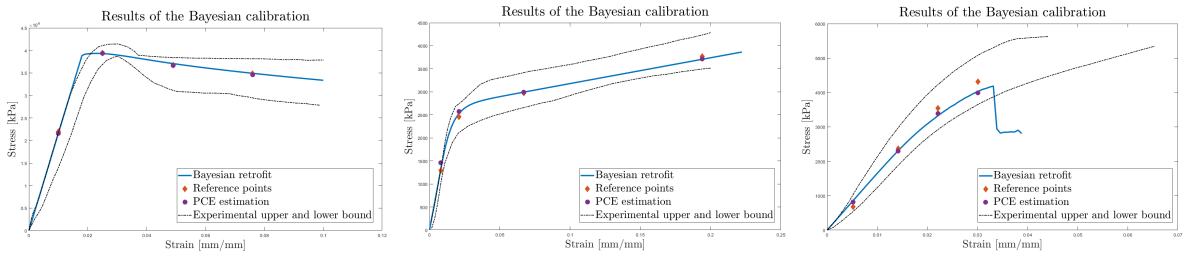

(a) Compression parallel to the grain

(b) Compression perpendicular to the grain

(c) Shear test

Figure 4: Stress-strain results of the characterization tests with the calibrated parameters compared to experimental results

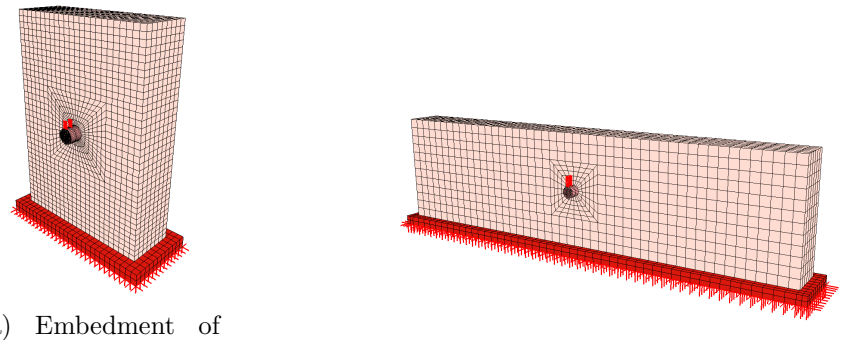

(a) Embedment of the dowel in the direction of the grain

(b) Embedment of the dowel in the direction perpendicular to the grain

Figure 5: Finite element models for dowel-embedment tests

Fig 5b and Fig. 5a show the finite element models used for the calculations. Boundary conditions are applied on the bottom steel plate. A vertical displacement-controlled load is applied on the ends of the dowel. The steel material for dowel follows a perfectly elastic-plastic rule with parameters $E = 210$GPa, $\nu = 0.3$ and $f_y = 200$MPa. An interface is set with coefficient of friction $\mu = 0.25$ on contact surfaces between wood and steel.

The resulting displacement-force curves are displayed on Fig. 6. Results show the model ability to reproduce the behaviour of experimental embedment tests. For both parallel and perpendicular loading, the numerical model qualitatively reproduces the experimental tests. The constitutive law combined with the calibrated material parameters give acceptable quantitative results for the parallel loading while the perpendicular loading does not quantitatively agree with the experimental results.

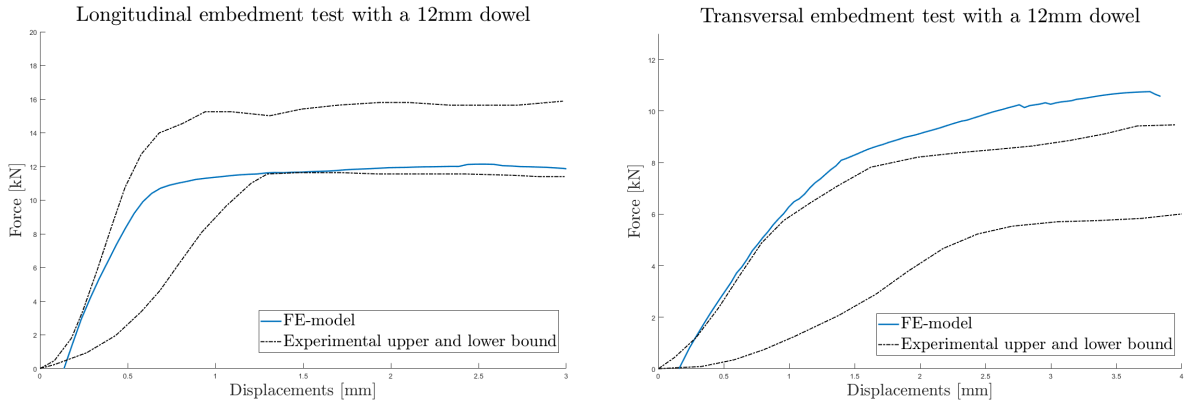

(a) In the direction parallel to the grain with a 12mm dowel

(b) In the direction perpendicular to the grain with a 12mm dowel

Figure 6: Force-displacment curves for the embedment tests

5 CONCLUSION

This paper presented a constitutive model for wood combining plastic theory and continuum damage mechanics. These nonlinear behaviours were implemented in the law to account for the ductile and brittle failure of wood. The law was implemented in a commercial software and validated on experimental results from the literature.

The calibration of the model parameters by means of a Bayesian inversion on results of compression of wood specimens was able to find a set of material parameters resulting in a good agreement between the numerical models and the experimental tests. Thus, it demonstrated the ability of the constitutive law to model the various non-linear behaviours of wood.

The material model and the calibration also succeeded in giving reasonable results for dowel-embedment test. This study suggests a method to combine constitutive model for wood with a parameter calibration method based on simple tests to simulate more complex wooden structures. Some further development on an additional failure mode in compression are to be pursued in order to improve the numerical models for a loading perpendicular to the fibres.

REFERENCES

[1] Rodney Hill and Egon Orowan. “A theory of the yielding and plastic flow of anisotropic metals”. In: *Proceedings of the Royal Society of London. Series A. Mathematical and Physical Sciences* 193.1033 (1948), pp. 281–297. DOI: 10.1098/rspa.1948.0045.

[2] Oscar Hoffman. “The Brittle Strength of Orthotropic Materials”. In: *Journal of Composite Materials* 1.2 (1967), pp. 200–206. DOI: 10.1177/002199836700100210.

[3] Stephen W. Tsai and Edward M. Wu. “A General Theory of Strength for Anisotropic Materials”. In: *Journal of Composite Materials* 5.1 (1971), pp. 58–80. DOI: 10.1177/002199837100500106. eprint: https://doi.org/10.1177/002199837100500106.

[4] Carmen Sandhaas, Jan-Willem van de Kuilen, and H. Blass. “Constitutive model for wood based on continuum damage mechanics”. In: *World Conference on Timber Engineering 2012, WCTE 2012* 1 (Jan. 2012).

[5] Mingqian Wang, Xiaobin Song, and Xianglin Gu. "Three-Dimensional Combined Elastic-Plastic and Damage Model for Nonlinear Analysis of Wood". In: *Journal of Structural Engineering* 144 (Aug. 2018). DOI: 10.1061/(ASCE)ST.1943-541X.0002098.

[6] Luis F. Sirumbal-Zapata, Christian Málaga-Chuquitaype, and Ahmed Y. Elghazouli. "A three-dimensional plasticity-damage constitutive model for timber under cyclic loads". In: *Computers & Structures* 195 (2018), pp. 47–63. DOI: https://doi.org/10.1016/j.compstruc.2017.09.010.

[7] Hooman Eslami, Laddu Bhagya Jayasinghe, and Daniele Waldmann. "Nonlinear three-dimensional anisotropic material model for failure analysis of timber". In: *Engineering Failure Analysis* 130 (2021), p. 105764. DOI: https://doi.org/10.1016/j.engfailanal.2021.105764.

[8] ZSOIL 2023. *A Windows-Based Tool offering a unified approach to numerical simulation of soil and rock mechanics, above & underground structures, excavations, soil-structure interaction and underground flow, including dynamics, thermal and moisture migration analysis*. GeoDev SARL.

[9] Stefano Marelli and Bruno Sudret. "UQLab: A Framework for Uncertainty Quantification in Matlab". In: *Vulnerability, Uncertainty, and Risk*, pp. 2554–2563. DOI: 10.1061/9780784413609.257. eprint: https://ascelibrary.org/doi/pdf/10.1061/9780784413609.257.

[10] A. Matzenmiller, J. Lubliner, and R.L. Taylor. "A constitutive model for anisotropic damage in fiber-composites". In: *Mechanics of Materials* 20.2 (1995), pp. 125–152. DOI: https://doi.org/10.1016/0167-6636(94)00053-0.

[11] J.C. Simo and J.W. Ju. "Strain- and stress-based continuum damage models—I. Formulation". In: *International Journal of Solids and Structures* 23.7 (1987), pp. 821–840. DOI: https://doi.org/10.1016/0020-7683(87)90083-7.

[12] Zdenek Bazant and Byung Oh. "Crack Band Theory for Fracture of Concrete". In: *Matériaux et Constructions* 16 (May 1983), pp. 155–177. DOI: 10.1007/BF02486267.

[13] C.L. Chow and June Wang. "An anisotropic theory of continuum damage mechanics for ductile fracture". In: *Engineering Fracture Mechanics* 27.5 (1987), pp. 547–558. DOI: https://doi.org/10.1016/0013-7944(87)90108-1.

[14] G. Duvaut and J. L. Lions. "Inequalities in mechanics and physics". In: *Grundlehren Der Mathematischen Wissenschaften* (1976). DOI: 10.1007/978-3-642-66165-5.

[15] V. Karagiannis, C. Málaga-Chuquitaype, and A.Y. Elghazouli. "Modified foundation modelling of dowel embedment in glulam connections". In: *Construction and Building Materials* 102 (2016). SHATIS 2013 : Research on Timber Materials and Structures, pp. 1168–1179. DOI: https://doi.org/10.1016/j.conbuildmat.2015.09.021.